Remeasurement of the Eötvös experiment - status and first results

Tóth, Gy., Szondy, Gy., Ván, P., Völgyesi, L., Barnaföldi, G., Deák, L., Égető, Cs., Fenyvesi, E., Harangozó, P., Gróf, Gy., Kiss, B., Lévai, P., Péter, G., Somlai, L.

BME Department of Geodesy and Surveying

FFK-2019 Tihany, 13.06.2019.

Overview

- gravity gradient bias in the EPF experiment
- current status and first results
- challenges

Origin of the gravity gradient bias

- A. changing sample geometry
- B. gravity field variation during the experiment

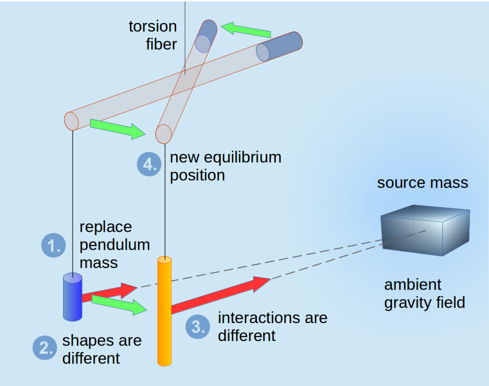

Simple formulation of the bias

- torque on the balance in E-W position is due to g_x North component
  - g_x must be integrated over sample volume to get the total force and torque
- linear vertical variation $g_x(z) = g_{xz}z$ ensures constant force for cylinders
- nonlinear vertical variation $g_x(z) = g_{xz}z + g_{xzz}z^2$ breaks constancy
- easy calculation shows sample height H dependence of arm rotation v:

$$v = -\frac{2}{\tau}ml\left(hg_{xz} + \left(h^2 + \frac{H^2}{12}\right)g_{xzz}\right)$$

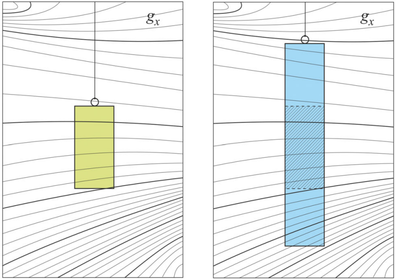

Magnitude of the gravity gradient bias

- bias in the equivalence parameter η depends on both sample shape (H) and gradient nonlinearity (g_{xzz}):

$$\eta_{bias} = -\frac{g_{xzz}}{12G \sin \epsilon}(H^2 - H'^2)$$

- more accurate calculation gives radius R dependence as well: $H^2/12 - R^2/4$
- sample geometry is known in the EPF experiment
- gravity field or its time variation is unknown

Gravity gradient bias in the EPF experiment

- Probable site of the original EPF experiment
  - Bod, Fischbach, Marx, Náray-Ziegler (1991) Figs. 6,7
  - small building with 4 windows facing South

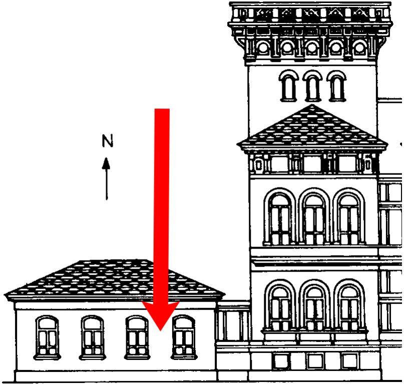

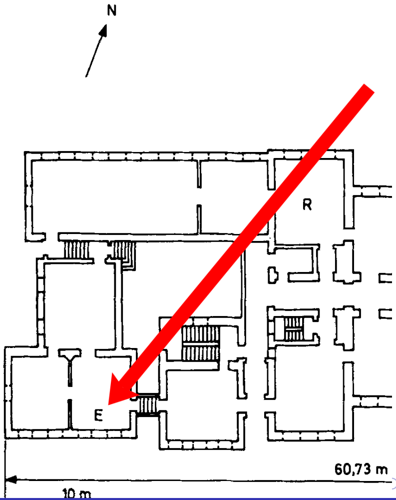

Guessing the gravity gradient bias

$$\eta_{bias} = -\frac{g_{xzz}}{12G\sin\epsilon}(H^2 - H'^2)$$

- g_{xzz} can be guessed from mass modeling
- $G\sin\epsilon$ is 1.69 mGal
- H^2 differences are known - e.g. Pt-Magnalium: $106\ cm^2$

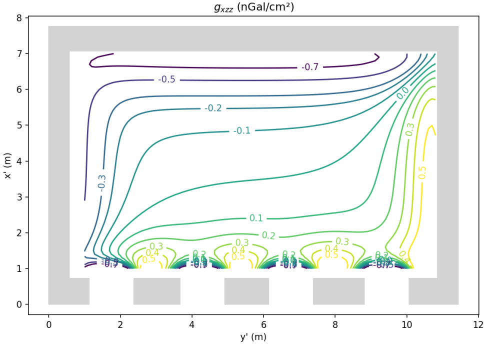

simple mass model of the EPF measurement: building with 4 windows made of bricks

g_{xzz} may easily reach $0.2\ nGal/cm^2$

$\rightarrow 1 \cdot 10^{-9}$ bias in $\Delta\eta_{Pt-Magnalium}$

What else can be said on this possible bias?

- Nobody knows precisely neither gravity nor its spatial and temporal variations at the EPF measurement site(s)
- Unfortunately this hypothesis does not explain the correlation found by Fischbach et al., but...
- ..but we can make a very interesting observation knowing the details of the different experimental protocols followed by EPF

Experimental protocols of EPF

- their published results were obtained initially with Method 2 and later with their refined Method 3
  - Method 2: one balance only, sample pairs were measured *subsequently*
  - Method 3: two balances of a double balance, sample pairs were measured *simultaneously*
  - Principal difference: temporal gravity field variation may have significantly biased Method 2, but not Method 3
- Observation: Temporal gravity field variation can make the sample geometry effect invisible in Method 2 but this is not the case for Method 3
- Conclusion: If our hypothesis is true, we must see the sample geometry effect in Method 3 results but we may not see this effect in Method 2 results
- Question: Do we actually see this difference in the EPF results?

Source multipole moments vs. EPF results

- q_{lm} multipole moments of the balance were calculated
  - main shape effect is linearly dependent on the $\Delta q_{31}/q_{31}$ moment ratio between the samples
- there is no dependence for Method 2 results, but we can see linear fit between error bars for Method 3 results
- details are in arXiv:1803.04720 and paper under review in EPJC

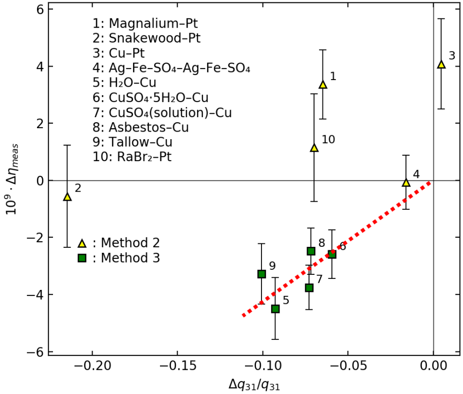

Consequences for the EPF remeasurement

- shape bias can be controlled by keeping the difference $H^2/12 - R^2/4$ constant
  - we use masses in our tests which obey this rule
- shape bias can be checked by breaking the above rule
  - we plan to use masses which break this rule to see the effect
- any remeasurement must keep gravity gradient bias under control

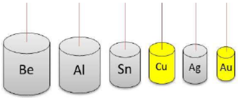

Gravity gradients at Jánossy Underground Laboratory (JFFL)

- Calculated from mass model of the laboratory
- Measured in-situ: U_{xz} = -15.2 E, U_{yz} = -14.4 E
- Expected vertical variation g_{xzz} is small
- Measured g_{xzz} is 0.051 nGal/cm^2

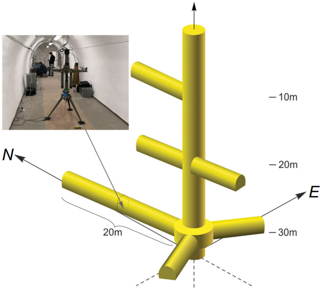

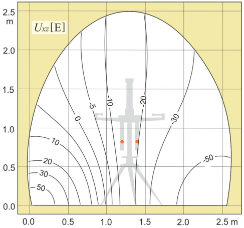

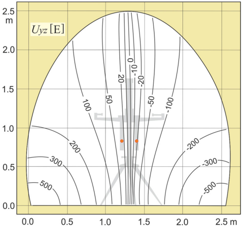

Current status of the remeasurement

- double Pekár balance (small original Eötvös G-2) installed at JFFL
- remote control and monitoring of the balance
- environment monitoring (thermal, air pressure, seismic)
- automated rotation and angular position control is nearly complete
- real-time automated monitoring of angular positions

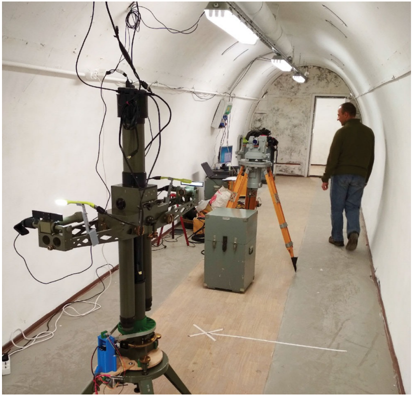

Tests for the solar gravity field

- Probably original idea of R. Eötvös

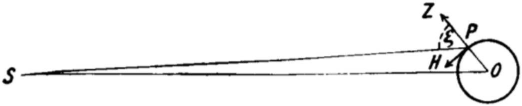

Fig. 4.

eine nach oben gerichtete vertikale Kraft (Fig. 4)

$$-Z = f\frac{M}{D^2}\cos\zeta - C\cos\zeta + fM\frac{a}{D^3}(2\cos^2\zeta - \sin^2\zeta)$$

- Published results for Pt-Magnalium pair

Beiträge zum Gesetze der Proportionalität usw. 49

7. Beobachtungen im Meridian zur Bestimmung der Differenz ($\varkappa - \varkappa'$) bezüglich der Sonnenanziehung.

Als Grundlage dient Gleichung (12) und die ihr vorangehenden Betrachtungen. Benützen werden wir das einfache Schwerevariometer, für welches

$$\Sigma m_a l_a \varkappa_a - \Sigma m_b l_b \varkappa_b = M_a l_a (\varkappa_a - \varkappa_b),$$

gesetzt

$$\vartheta = \vartheta_0 - \frac{1}{\tau}\left(f_0 \frac{M}{D^2}\right) M_a l_a (\varkappa_a - \varkappa_b) \sin\zeta \sin A,$$

für die Sonnenanziehung

$$f_0 \frac{M}{D^2} = 0{,}586$$

Wir haben dann aus den Beobachtungen der ersten Versuchsreihe:

$$n' - n = -0{,}062,$$

aus den Beobachtungen der zweiten Versuchsreihe:

$$n' - n = -0{,}046.$$

Wollten wir unsere Berechnung auf eine einzige Versuchsreihe begründen, also die Formel (a) benützen, so ergebe sich

$$\varkappa_{Magnalium} - \varkappa_{Pt} = -0{,}018 \cdot 10^{-6}.$$

Mit Ausschluß jener störenden Einflüsse, welche Schwankungen von täglicher Periode bewirken, also mit Benutzung der Resultate beider Versuchsreihen und der Formel (b) erhalten wir aber richtiger

$$\varkappa_{Magnalium} - \varkappa_{Pt} = +0{,}006 \cdot 10^{-6}.$$

- Sun’s gravity was first tested on Cu-Au pair
  - the upper masses of both balances of the Pekár balance are Au
  - 6.5 days in 0° azimuth (N) with Cu-Au
  - 13 days in 180° azimuth (S) with Cu-Au (data gaps)

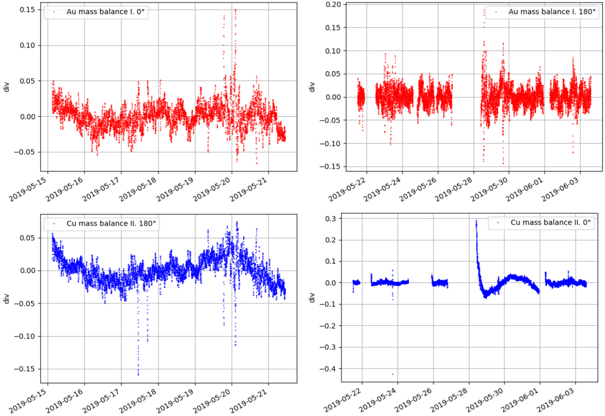

Tests for the solar gravity field

- Sun’s gravity was next tested on Al-Au pair
  - 7+ days in 0° azimuth with Al-Au pair
  - quadratic drift was removed
  - data were downsampled to 1 min

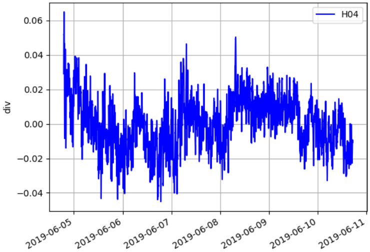

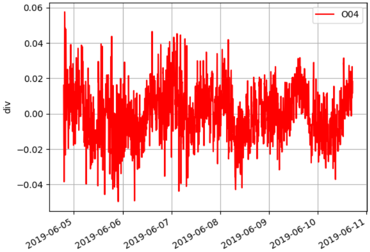

Data processing

- Method by Roll, Krotkov, Dicke (1964)
  - least-squares fitting of readings n as function of true local solar time t ($t = 0$ at noon):
  - $n(t) = S\sin(t) + C\cos(t) + K$
  - calculation of η from amplitude S

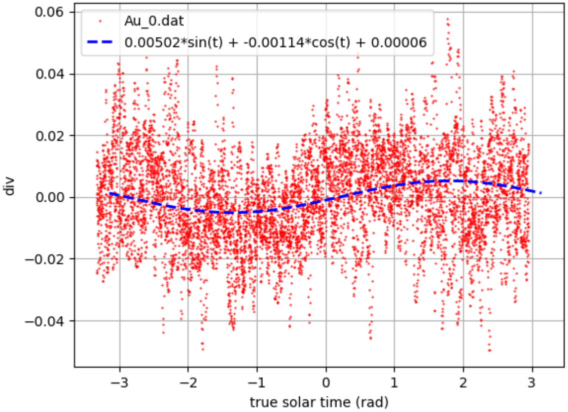

Preliminary results of our solar gravity tests

- Estimated errors are at level $2 \cdot 10^{-9}$ (from non-null results on Au-Au)
  - low-frequency noise limits precision
  - must correct for pressure effects
  - analyze possible thermal effects

measurement period	material	η
05.15-05.20.	Cu	$0.60 \cdot 10^{-9}$
05.15-05.20.	Au	$1.15 \cdot 10^{-9}$
05.21-06.04.	Cu	$-1.85 \cdot 10^{-9}$
05.21-06.04.	Au	$-1.01 \cdot 10^{-9}$
06.04-06.11.	Al	$1.50 \cdot 10^{-9}$
06.04-06.11.	Au	$1.86 \cdot 10^{-9}$

Frequency analysis of angular positions

- residuals of quadratic fits were analyzed
  - strong 3 h component - temperature signal?
  - low frequency components dominate

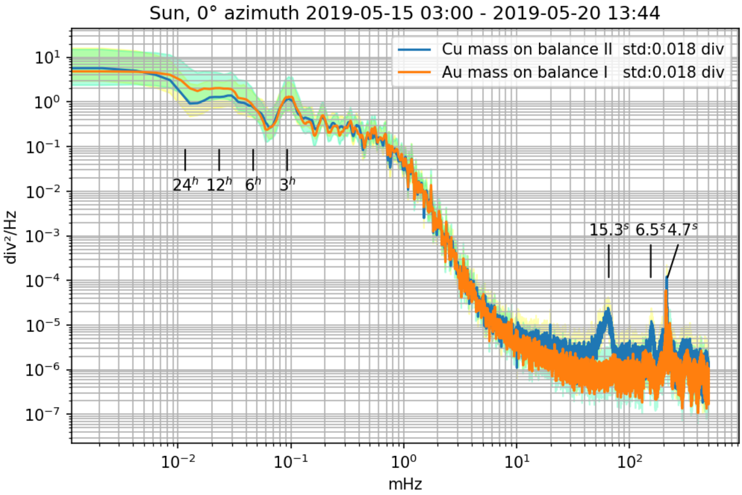

Frequency analysis of angular positions

- cumulative PSD of residuals
  - strong signal contribution in the 5 min - 3 h range
  - damped torsional eigenfrequency is ≈ 30 min

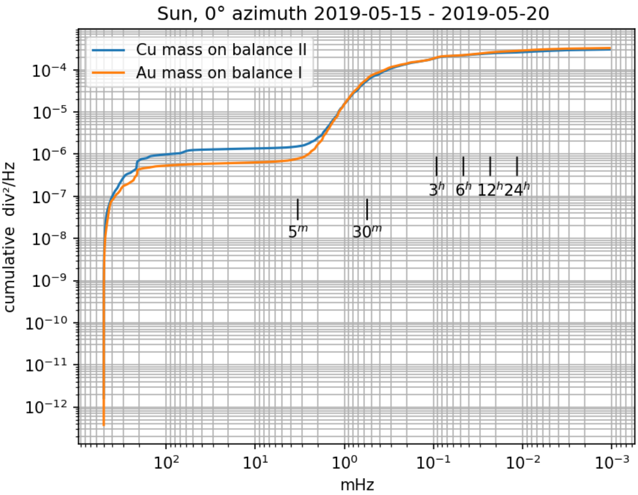

Challenges

- even if we do not aim "record precision" with our balance, we face the following challenges:
  - jump-like rotation changes by the load of torsion wire
  - sensitivity of the balance to vibrations
  - atmospheric air pressure influence
  - high accuracy determination of balance beam orientation

Jump-like rotation changes by the load of torsion wire

- Jumps occur only after an extended time of unloading
- No such jumps when the wires are almost constantly loaded

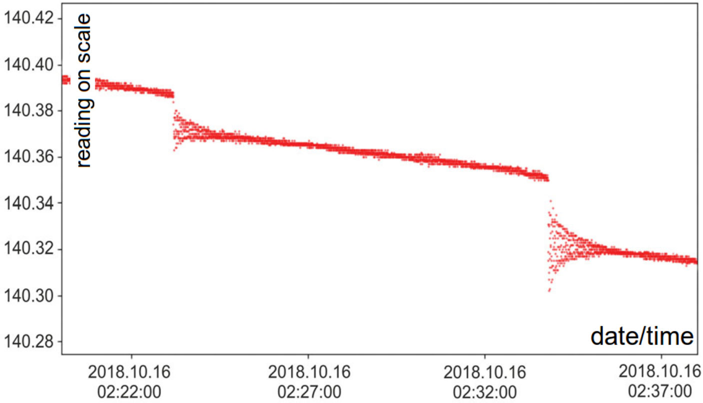

Wire drift and puzzling correlation

- Initial quadratic drift is 0.01 div/h but becomes almost linear after 1 day and decreases to 0.005 div/h (2 μrad/h) and below
- drift corrected residuals show marked (anti)correlation that puzzled us for a long time

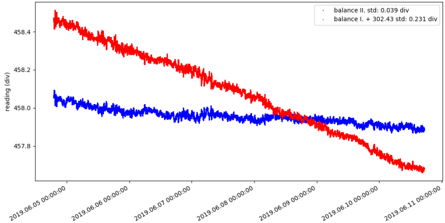

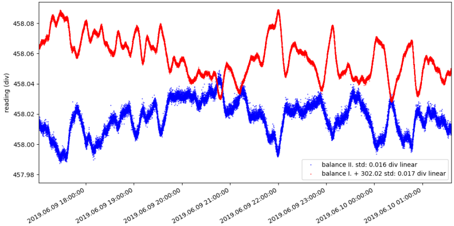

Sensitivity of the balance to vibrations of the suspension point

- Speake and Gillies (1987) discusses this shorly and refers to a paper by Karagioz et al. (1975)
- "dumb-bell effect": simple pendulum oscillation can apply torques to the torsion mode of the pendulum
- physical mechanism: reduction of the kinetic energy by the lining up of the dumb-bell with the axis of rotation
- simulated response of a simple balance to its suspension point vibration with amplitude 1 μm and frequency 10 Hz

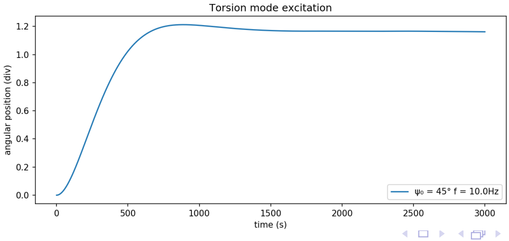

Torsion balances for operational earthquake forecasting

- The effect of the reaction of a gravitational variometer (GV) on vibrations due to seismic activity was discovered at the end of 1970's practically by chance at Russia (Volfson et al. 2010)
- The GV's response was observed in case of an extremely remote signal source, as a rule, several tens of hours before a cataclysm (Kalinnikov et al., 1992)
- The balance tends to the maximally possible energy absorption during resonant reciprocating horizontal motion of the top of the suspension (Kalinnikov, 1990).
- At the end of the 1980's, 18 pairs of GVs were mounted at 7 seismic stations of Kazakhstan and their records were fixed on a continuous basis for the past 15 years (Khaidarov et al., 2003)

Torsion balances for operational earthquake forecasting

- Typical curve of GV signals vs. seismic activity in the area of the oncoming earthquakes (Volfson et al. 2011)

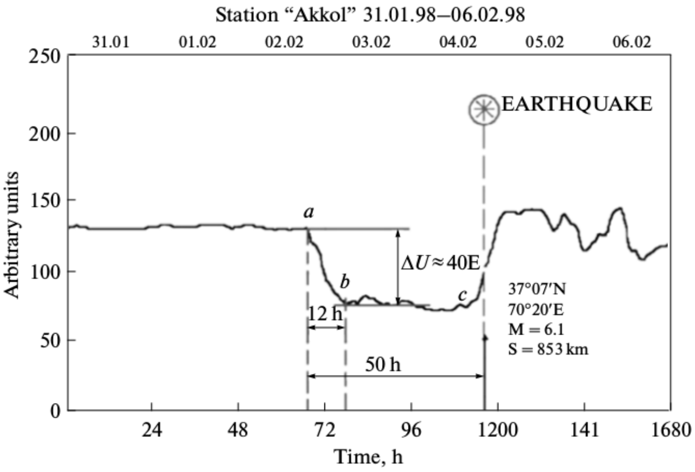

- Surface waves of the M = 4.3 Serbian shallow earthquake event at 12.03.2018 06:34.
- event registered by the torsion balance at JFFL
- seismogram of the Kövesligethy Radó Seismological Observatory

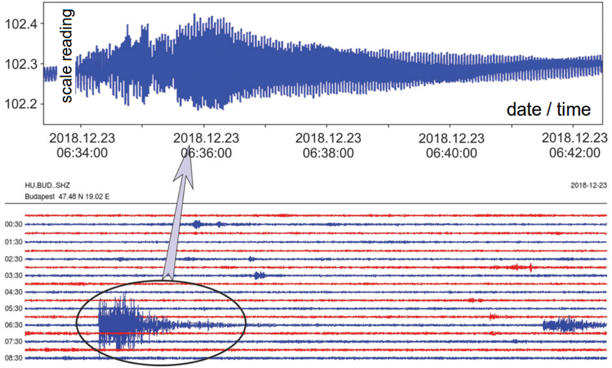

Air pressure monitoring

- Pressure variations are monitored in situ with Bosch BME280 sensor
- Environmental data are monitored at the top of a nearby building
- Pressure variations show good correlation

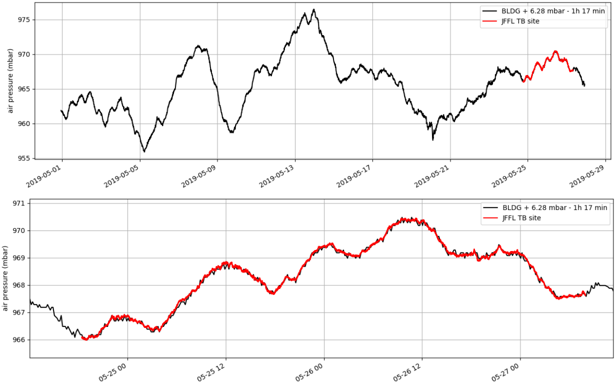

Air pressure monitoring

- Spectral analysis of air pressure signal
- semi-diurnal atmospheric tidal component is visible
- diurnal component is not clear

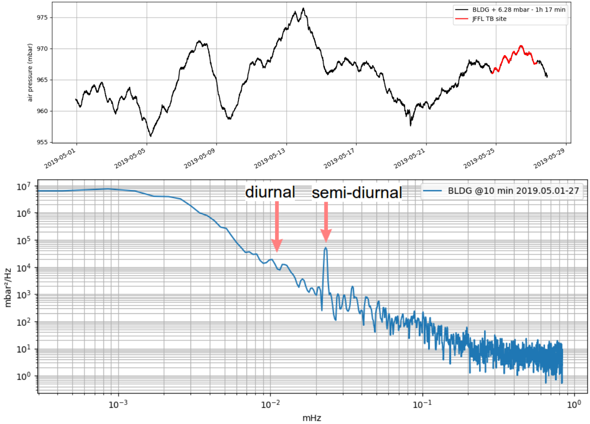

Correlation of angular position with air pressure

- Bandpass filtered (2 min - 60 min) air pressure shows good (anti)correlation with angular position of the balances
- effect strongly depends on the azimuth of the balance's arm
- obvious possibility to reduce noise level

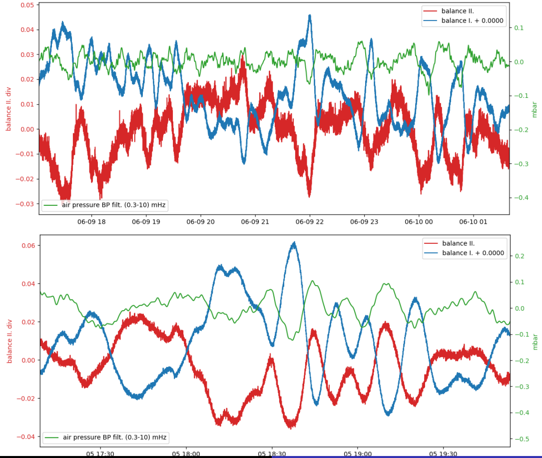

Similar correlation has already been found...

- Operational research with wideband gravitational gradiometers (WBG) at Tula University by S.A. Shopin
- intended to the measurement of nonhomogeneous gravity field gradient by registration of the angular position of the torsion system beam

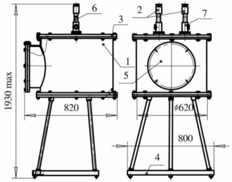

Figure 4. System case-screen: 1 – working volume of the case; 2 – fastening and regulation device of the torsion system; 3 – case cover; 4 – instrument basement; 5 – cover of the working window; 6 – duct;7 – duct stand

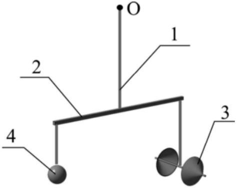

Рис. 1. Крутильная система прибора ШГМ: O — точка подвеса крутильной системы; 1 — нить подвеса; 2 — коромысло; 3 — груз сложной формы; 4 — груз-противовес

- WBG signals vs. 1-50 mHz bandpass filtered air pressure signal
- strong correlation with bandpass filtered atmospheric pressure signal found (Shopin, 2014)
- working hypothesis: torsional systems work as band-pass filters for variations in atmospheric pressure

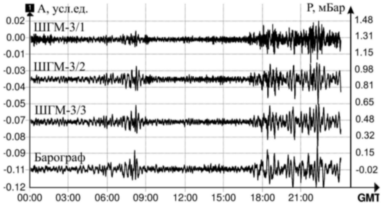

Рис. 13. Полосовая фильтрация данных ШГМ-3 и барографа за 24.08.2013

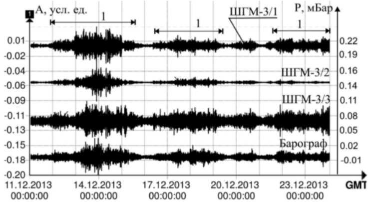

Рис. 15. Фильтрация данных ШГМ-3 и барографа за период 11.12.–23.12.2013 г.: 1 — интервалы шум-сигналов

Plans

- correction/compensation of measurements for environmental effects (pressure, temperature, vibrations, magnetic field)
- measurements to test equivalence in the Earth's gravity field
  - continuous rotation of the balance in N,E,S,W azimuths
  - accurate rotation and angular position determination (~10 arc seconds) is required
  - accurate (0.1 E) gravity gradient determination is necessary
- check gravity gradient bias using test masses of non-optimal shapes

The End

- thresholding: Sauvola binarization
- connected component analysis
- bounding boxes: scale division marks, figures
- merging bounding boxes

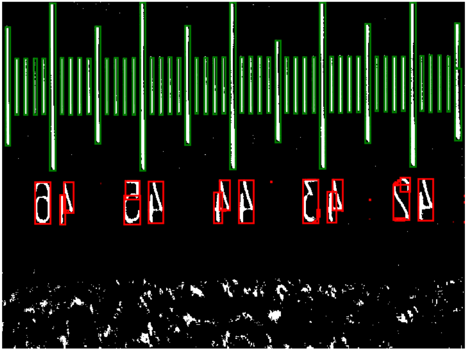

Image analysis

- calculate distance between scale divisions
- sequential labeling of scale divisions
- calculate postions of 10-marks
- digit recognition based on feature space distances (similiarity measure)
- calculate average reading to image center (std: 0.0025 div)

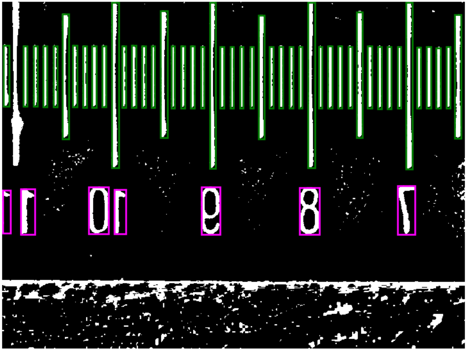

Temperature sensor data

- mounted at JFFL TB
- human "interventions" are seen as sharp jumps
- for flat part variation is $\pm 0.02°$C
- digitization error limits accuracy

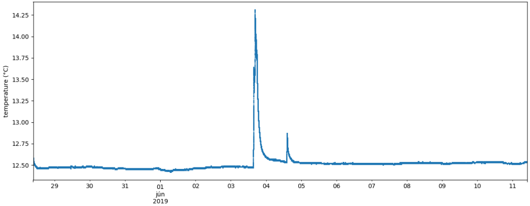

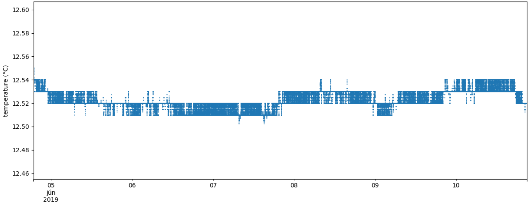

Spectrum of temperature sensor data

- 24, 6 and 3 hour components are visible

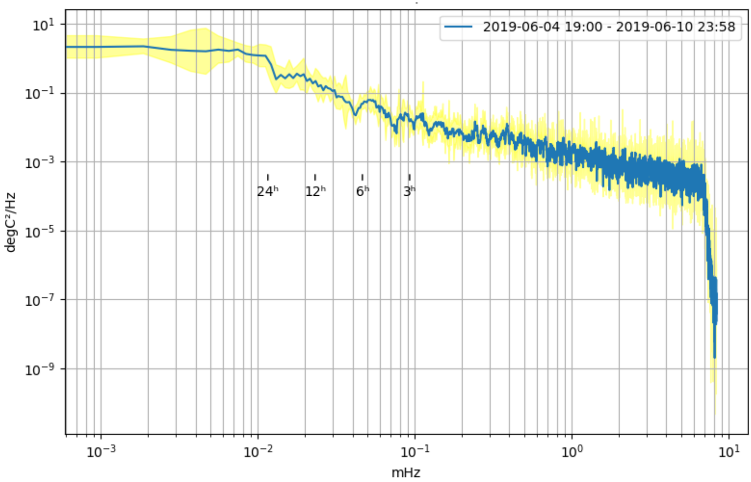

Accuracy analysis

- errors of angular positions are simulated as AR(1) process with 1 min sampling with lag-1 autocovariance of 0.4 (decorrelation time: 130 s) with standard deviation: 0.0025 div
- length of data: 6 days
- $\eta = 1 \cdot 10^{-9}$ - estimated: $0.89 \cdot 10^{-9}$
- $\eta = 5 \cdot 10^{-10}$ - estimated: $4.2 \cdot 10^{-10}$
- $\eta = 1 \cdot 10^{-10}$ - estimated: $0.7 \cdot 10^{-10}$